

**Electronic Supplementary Information**  
**for**  
**A Novel Acid-Base Bifunctional Catalyst of ZSM-5@Mg<sub>3</sub>Si<sub>4</sub>O<sub>9</sub>(OH)<sub>4</sub> with**  
**Core/Shell Hierarchical Structures and Superior Activities in Tandem**  
**Reactions†**

Darui Wang, Bo Wang, Yu Ding, Haihong Wu and Peng Wu\*

*Shanghai Key Laboratory of Green Chemistry and Chemical Processes, School of Chemistry and Molecular Engineering, East China Normal University, North Zhongshan Rd. 3663, Shanghai 200062, China*

## **EXPERIMENTAL SECTION**

### **Chemicals**

All chemicals and reagents were obtained from commercial suppliers and used without further purification: tetraethyl orthosilicate (Sigma-Aldrich, ≥98% Reagent Grade), tetrapropylammonium hydroxide (TCI, 25 wt% in water), silica sol (Sigma-Aldrich, 30 wt%), piperidine (Aladdin, ≥99.5% analytical standard), aluminum sulfate octadecahydrate (Aladdin, 98.0% - 102.0% ACS reagent), sodium hydroxide (Alfa Aesar, 98.0% flake), ammonium chloride (Alfa Aesar, ≥98%), aqueous ammonia solution (Sinopharm Chemical Reagent Co., Ltd., 28 wt%), magnesium nitrate (Sinopharm Chemical Reagent Co., Ltd., ≥99.0% analytical standard), toluene (Sinopharm Chemical Reagent Co., Ltd., ≥99.5% analytical standard), benzaldehyde dimethylacetal (TCI, ≥98.0% analytical standard), malononitrile (TCI, ≥98.0% analytical standard), ethyl cyanoacetate (TCI, ≥99.0% analytical standard), anhydrous ethanol (Sinopharm Chemical Reagent Co., Ltd., ≥99.7% analytical standard), Air and N<sub>2</sub> gases (99.999 vol.%) were supplied by Shanghai Pujiang Specialty Gases Co., Ltd.

### **Synthesis of ZSM-5 zeolite**

ZSM-5 zeolite was synthesized with the assistance of active seeds. The active seeding gel was prepared according to the procedures reported previously.<sup>1</sup> Tetraethyl orthosilicate (TEOS) was dropped into the solution containing water and tetrapropylammonium hydroxide (TPAOH, 25 % aqueous solution). After homogenizing at 80 °C for 2 h, the synthetic gel with a molar composition of 1.0 TEOS : 0.15 TPAOH : 14 H<sub>2</sub>O was introduced into a Teflon-lined steel autoclave and aged at 120 °C for 3 h. After cooling, the obtained seeding gel was directly used for the synthesis of ZSM-5 zeolites without any treatment.

ZSM-5 zeolite was synthesized from piperidine (PI) as structure directing agent, silica sol (30 wt.% SiO<sub>2</sub>), aluminum sulfate and sodium hydroxide. Sodium hydroxide and aluminum sulfate were first dissolved in the aqueous solution of piperidine. Silica sol and active seeding gel were then dropped into the above solution and further stirred for 30 minutes, forming a gel composition of 1.0 SiO<sub>2</sub> : 0.0125 Al<sub>2</sub>O<sub>3</sub> : 0.2 PI : 0.05 Na<sub>2</sub>O : 25 H<sub>2</sub>O. SiO<sub>2</sub> in the active seeding gel accounted for 1 % of the whole SiO<sub>2</sub> in gel. The gel was crystallized in a Teflon-lined steel autoclave at 170 °C for 72 h. The ZSM-5 product was collected by filtration followed by washing with distilled water several times, dried at 100 °C overnight, and then calcined in air at 550 °C for 6 h to remove the organic template. The resulting ZSM-5 was brought into ammonium form *via* three consecutive exchanges in 1 M ammonium chloride solution at 80 °C for 2 h. After filtration, washing and drying overnight at 110 °C, the ammonium ion-exchanged zeolite was subsequently calcined at 550 °C for 6 h to give proton-type H-ZSM-5.

#### **Synthesis of hierarchically acid-base bifunctional material of ZSM-5@Mg<sub>3</sub>Si<sub>4</sub>O<sub>9</sub>(OH)<sub>4</sub>**

ZSM-5@Mg<sub>3</sub>Si<sub>4</sub>O<sub>9</sub>(OH)<sub>4</sub> was prepared through a simple hydrothermal process. In a typical synthesis, Mg(NO<sub>3</sub>)<sub>2</sub>·6H<sub>2</sub>O (0.158 - 0.475 g), NH<sub>4</sub>Cl (0.535 g) and NH<sub>3</sub>·H<sub>2</sub>O (0.91 g, 28%) were added under stirring in distilled water (70 g). As prepared H-ZSM-5 powder (0.3 g) was then added to the above solution and ultrasonicated for 30 min to form a uniform suspension, then the mixture was transferred to a Teflon autoclave (100 mL) and heated to 80 - 140 °C for 3 h. After the autoclave was cooled to room temperature, the resulting green precipitates were collected and washed several times with distilled water and absolute ethanol. The final products were dried

under vacuum at 60 °C for 4 h. And the Mg content for resultant ZSM-5@Mg<sub>3</sub>Si<sub>4</sub>O<sub>9</sub>(OH)<sub>4</sub> was 5.0 - 15.0 wt% calculated by ICP analysis.

### **Synthesis of MgO/ZSM-5 by wetness impregnation method**

In a typical synthesis, Mg(NO<sub>3</sub>)<sub>2</sub>·6H<sub>2</sub>O (1.057 g) was dissolved in distilled water (1 g), and then the solution was slowly dropped onto H-ZSM-5 zeolite (1 g) with continuous stirring at ambient temperature for a total of 4 h. After completing this procedure, the material was firstly dried overnight at ambient temperature and then further at 110 °C for 12 h, then the material was calcined at 500 °C for 4 h to obtain MgO/ZSM-5. Mg content for the resultant MgO/ZSM-5 was 9.9 wt% as determined by ICP analysis.

### **Catalytic reactions**

The one-pot tandem deacetalization-Knoevenagel condensation reaction was carried out at 90 °C in toluene under N<sub>2</sub>. In a type run, the catalyst (50 mg), benzaldehyde dimethylacetal (7.5 mmol), malononitrile or ethyl cyanoacetate (5 mmol), H<sub>2</sub>O (5 mmol) and toluene (2 mL) were mixed in a flask connected to a cooling condenser. Then the flask was immersed in a water bath equipped with a magnetic stirrer. The products were separated by filtration and analyzed on a gas chromatograph (Shimadzu 2014, FID detector) equipped with a 30 m OV-1 capillary column.

Reusability of the catalyst was studied as follows. After the first run, the catalyst was washed three times with anhydrous ethanol, dried at 60 °C in air and reused for the next run. The above procedure was repeated eight times.

### **Characterization methods**

Powder X-ray diffraction (XRD) was employed to check the structure and crystallinity of the zeolites. The XRD patterns were collected on a Rigaku Ultima IV diffractometer using Cu K $\alpha$  radiation at 35 kV and 25 mA in the 2 $\theta$  angle range of 5 - 80° using a step size of 0.02° and at a scanning speed of 10° min<sup>-1</sup>.

Nitrogen gas adsorption measurements were carried out at -196 °C on a BEL-MAX gas/vapor adsorption instrument. The samples were evacuated at 300 °C for at least 6 h before adsorption. The *t*-plot method was used to discriminate between micro- and mesoporosity. The surface areas

were calculated by the Brunauer-Emmett-Teller (BET) method. The mesopore size distribution was obtained by the BJH model from the adsorption branches of the isotherms.

Si, Al and Mg contents were determined by inductively coupled plasma emission spectrometry (ICP) on a Thermo IRIS Intrepid II XSP atomic emission spectrometer.

The IR spectra were collected on a Nicolet Nexus 670 FT-IR spectrometer in absorbance mode at a spectral resolution of  $2\text{ cm}^{-1}$  using KBr technique (2 wt% wafer).

The temperature-programmed desorption of ammonia ( $\text{NH}_3$ -TPD) and the temperature-programmed desorption of carbon dioxide ( $\text{CO}_2$ -TPD) were performed on Micrometrics tp-5080 equipment equipped with a thermal conductivity detector (TCD) detector. The TPD profile was recorded at a heating rate of  $10\text{ }^\circ\text{C min}^{-1}$  from  $100\text{ }^\circ\text{C}$  to  $600\text{ }^\circ\text{C}$ .

The thermogravimetric and differential thermal analyses (TG-DTA) were performed on a METTLER TOLEDO TGA/SDTA851<sup>e</sup> apparatus from  $25\text{ }^\circ\text{C}$  to  $800\text{ }^\circ\text{C}$  at a heating rate of  $10\text{ }^\circ\text{C min}^{-1}$  in air.

Solid-state NMR spectra were recorded on a VARIAN VNMRS-400WB NMR spectrometer.

X-ray photoelectron spectra (XPS) were recorded on a Thermo VG Escalab 250 X-ray photoelectron spectrometer at a pressure of about  $2 \times 10^{-9}\text{ Pa}$  with Al  $K\alpha$  X-rays as the excitation source.

Scanning electron microscopy (SEM) was performed on a Hitachi S-4800 microscope to determine the crystal morphology.

Transmission electron microscopy (TEM) images were collected on a Tecnai G<sup>2</sup> F30 microscope. The sample was firstly made suspension in ethanol by ultrasonication, and a drop of such suspension was deposited onto a holey carbon foil supported on a copper grid.

**Table S1** The textural properties of the pristine ZSM-5, ZSM-5@Mg<sub>3</sub>Si<sub>4</sub>O<sub>9</sub>(OH)<sub>4</sub> and MgO/ZSM-5.

Catalysts	S <sub>BET</sub> <sup>a</sup> (m <sup>2</sup> g <sup>-1</sup> )	S <sub>ext</sub> <sup>b</sup> (m <sup>2</sup> g <sup>-1</sup> )	V <sub>tot</sub> <sup>c</sup> (cm <sup>3</sup> g <sup>-1</sup> )	V <sub>micro</sub> <sup>b</sup> (cm <sup>3</sup> g <sup>-1</sup> )	V <sub>meso</sub> <sup>d</sup> (cm <sup>3</sup> g <sup>-1</sup> )	Mg <sup>e</sup> (wt%)
ZSM-5	378	31	0.27	0.17	0.10	0
ZSM-5@Mg <sub>3</sub> Si <sub>4</sub> O <sub>9</sub> (OH) <sub>4</sub>	474	193	0.40	0.14	0.26	10.0
MgO/ZSM-5	251	16	0.16	0.10	0.06	9.9

<sup>a</sup> Obtained by BET method.

<sup>b</sup> Obtained by *t*-plot method.

<sup>c</sup> Given by the adsorption amount at P/P<sub>0</sub> = 0.99.

<sup>d</sup> V<sub>meso</sub> = V<sub>tot</sub> - V<sub>micro</sub>.

<sup>e</sup> Mg contents were analyzed by ICP.

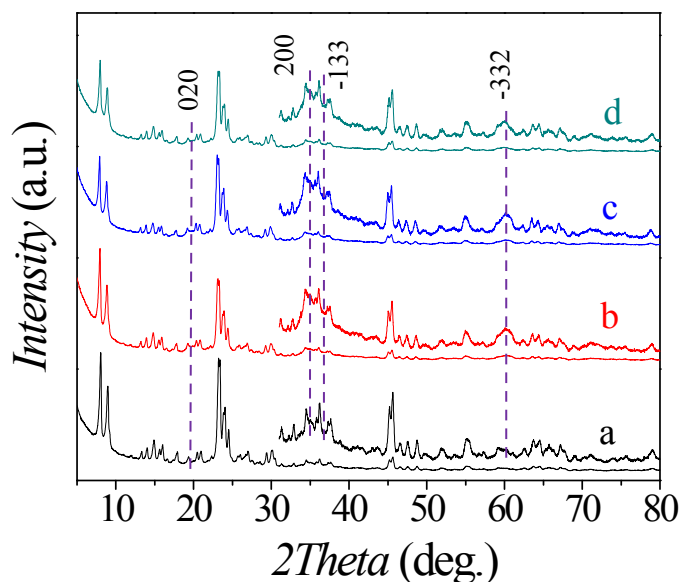


**Fig. S1** XRD patterns of ZSM-5@Mg<sub>3</sub>Si<sub>4</sub>O<sub>9</sub>(OH)<sub>4</sub> obtained at different temperature: 80 °C (a), 100 °C (b), 120 °C (c) and 140 °C (d).

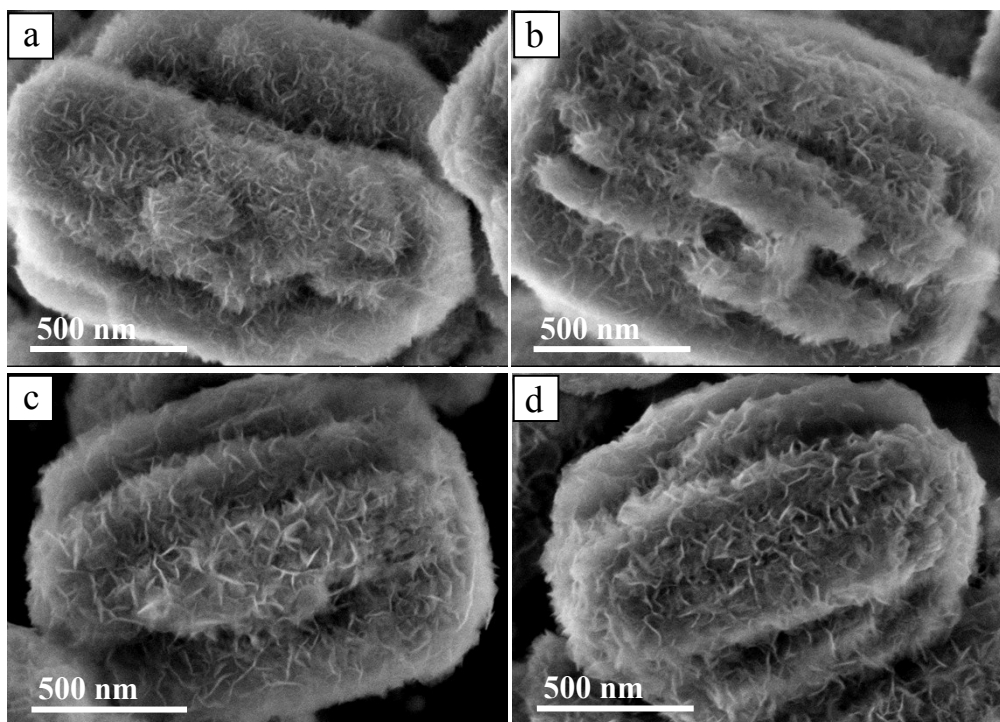


**Fig. S2** SEM images of ZSM-5@Mg<sub>3</sub>Si<sub>4</sub>O<sub>9</sub>(OH)<sub>4</sub> obtained at different temperature: 80 °C (a), 100 °C (b), 120 °C (c) and 140 °C (d).

To investigate the effect of reaction temperature on the formation of hierarchical ZSM-5@Mg<sub>3</sub>Si<sub>4</sub>O<sub>9</sub>(OH)<sub>4</sub> composite materials, we monitored the reactions at the same time of 3 h but changing the reaction temperature. At lower temperatures of 80 °C and 100 °C, the flower-like nanosheets were shorter, tighter and closely aggregated each other. At reaction temperature of 80 °C, only a small amount of flower-liked nanosheets were coated on the ZSM-5, and Mg content was 7.2 wt% according ICP analysis. At higher temperatures of 120 °C and 140 °C, the nanosheets exhibited a much clearer morphology, and became less aggregated. The Mg content was leveled off at 120 °C, suggesting that the reaction was complete. The maximum loading of 10.0 wt% was close to the amount of Mg source added. Therefore, we deem that well-structured ZSM-5@Mg<sub>3</sub>Si<sub>4</sub>O<sub>9</sub>(OH)<sub>4</sub> materials can be prepared by hydrothermal reaction under optimal temperature and time of 120 °C and 3 h, respectively.

Correspondingly, the intensity of peaks indexed as magenium silicate in XRD patterns (Fig. S1) increased with raising reaction temperature, while the intensity of peaks due to MFI zeolite topology decreased.

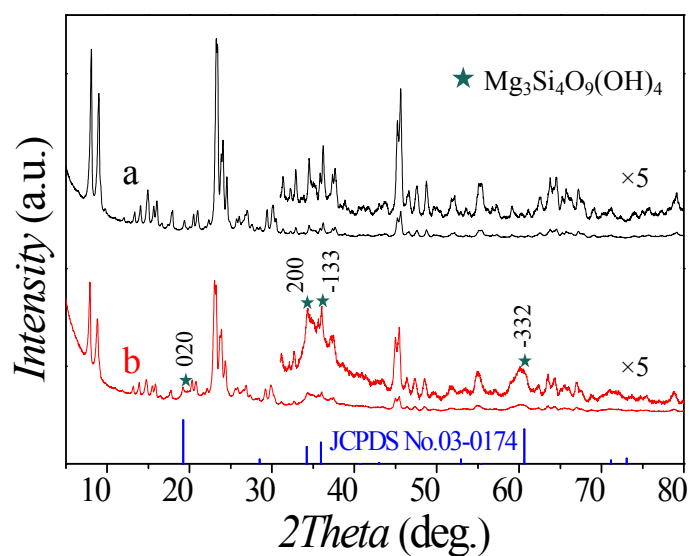


**Fig. S3** XRD patterns of the pristine ZSM-5 (a), ZSM-5@Mg<sub>3</sub>Si<sub>4</sub>O<sub>9</sub>(OH)<sub>4</sub> (b) and standard Mg<sub>3</sub>Si<sub>4</sub>O<sub>9</sub>(OH)<sub>4</sub>.

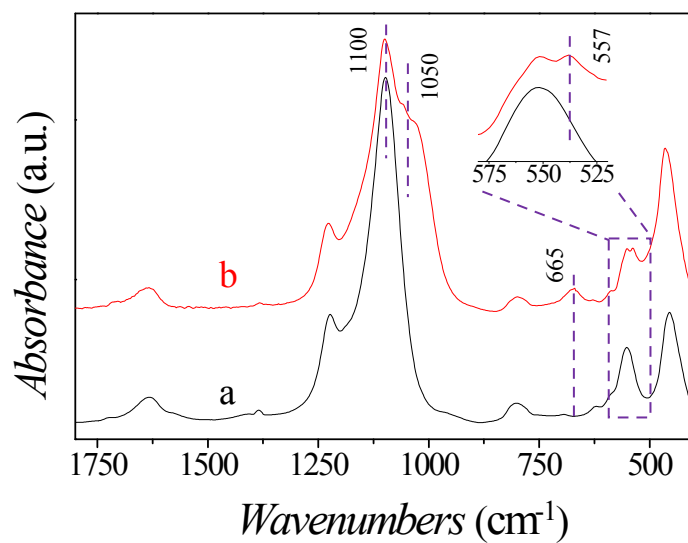


**Fig. S4** FT-IR spectra of the pristine ZSM-5 (a) and ZSM-5@Mg<sub>3</sub>Si<sub>4</sub>O<sub>9</sub>(OH)<sub>4</sub> (b). The inset shows the enlarged region for Si-O-Mg stretching vibration.

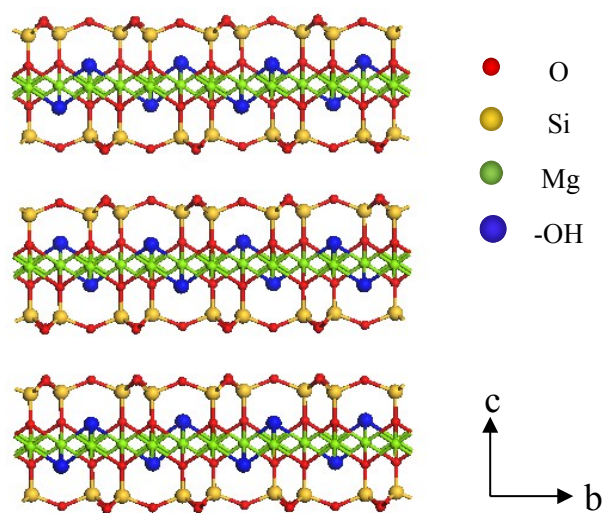


**Fig. S5** Three-dimensional images of the magnesium silicate layer structure.

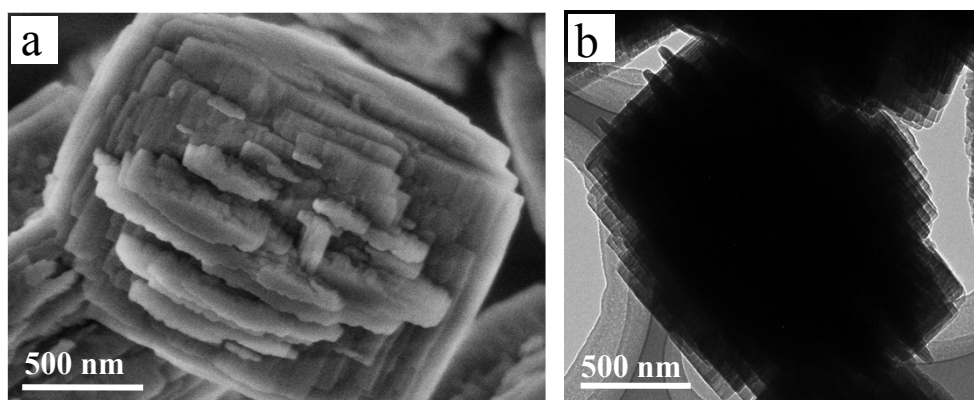


**Fig. S6** SEM and TEM images of the pristine ZSM-5.

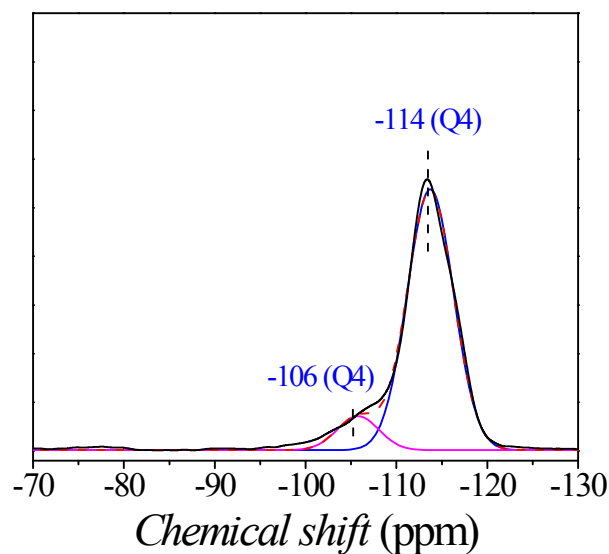


**Fig. S7** Solid state  $^{29}\text{Si}$  NMR spectra of the pristine ZSM-5.

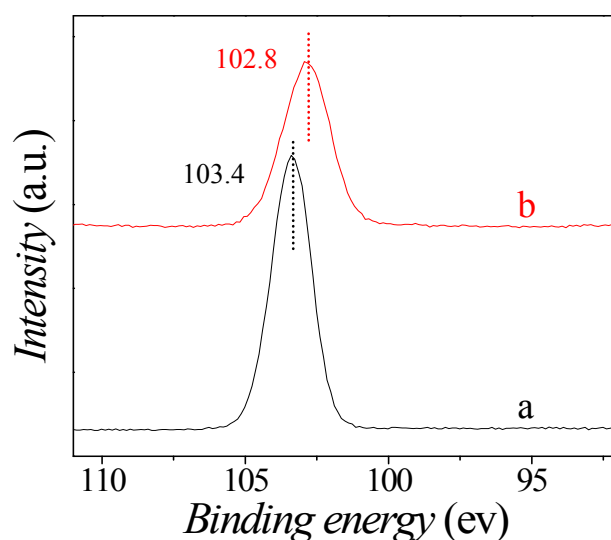


**Fig. S8** The Si 2p XPS spectrum of pristine ZSM-5 (a) and ZSM-5@ $\text{Mg}_3\text{Si}_4\text{O}_9(\text{OH})_4$  (b).

According to XPS analysis, Si/Al molar ratios were 42 and 260 for the pristine ZSM-5 surface and ZSM-5@ $\text{Mg}_3\text{Si}_4\text{O}_9(\text{OH})_4$  surface, respectively. This result indicated that  $\text{Mg}^{2+}$  reacted with silica species dissolved from ZSM-5 crystal surface selectively, while aluminium entered the solution directly. And Si/Mg molar ratio was approximately 1.4 for ZSM-5@ $\text{Mg}_3\text{Si}_4\text{O}_9(\text{OH})_4$  surface, which was in agreement with the structure of  $\text{Mg}_3\text{Si}_4\text{O}_9(\text{OH})_4$ .

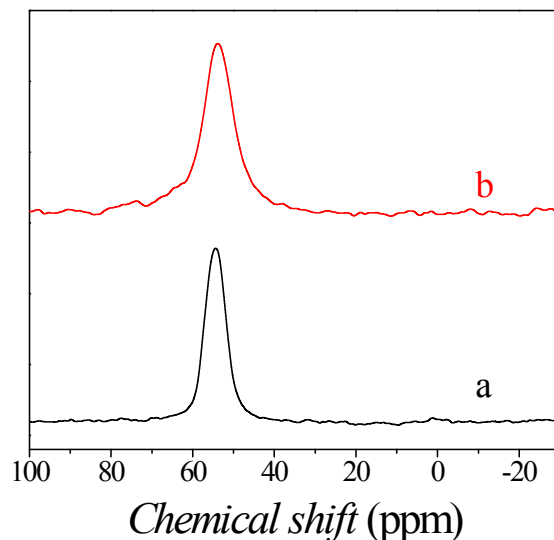


**Fig. S9** The  $^{27}\text{Al}$  MAS NMR spectra of pristine ZSM-5 (a) and ZSM-5@ $\text{Mg}_3\text{Si}_4\text{O}_9(\text{OH})_4$  (b).

The  $^{27}\text{Al}$  MAS NMR spectra of the pristine ZSM-5 showed only one signal of tetrahedral Al at 58 ppm, but no resonance at 0 ppm due to octahedral Al, which means that the Al ions were incorporated predominantly in the framework position. After incorporating  $\text{Mg}_3\text{Si}_4\text{O}_9(\text{OH})_4$ , ZSM-5@ $\text{Mg}_3\text{Si}_4\text{O}_9(\text{OH})_4$  also showed only one signal of tetrahedral Al at 58 ppm as pristine ZSM-5, but the signal became broader. This implied that the microenvironment of Al became more asymmetric in coordination states. According to the ICP analyses, the Si/Al molar ratios for the pristine ZSM-5 and ZSM-5@ $\text{Mg}_3\text{Si}_4\text{O}_9(\text{OH})_4$  precursors were 40.5 and 41.0, respectively. According to the unchanged Si/Al ratio and above broadened signal, we can assume that Al was also extracted from ZSM-5 along with the silica dissolution and Al was incorporated into the magnesium silicate phase.

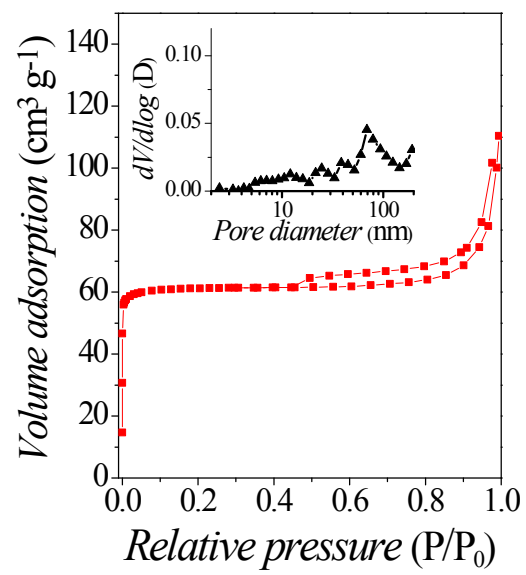


**Fig. S10**  $N_2$  adsorption/desorption isotherm and BJH pore size distribution of MgO/ZSM-5.

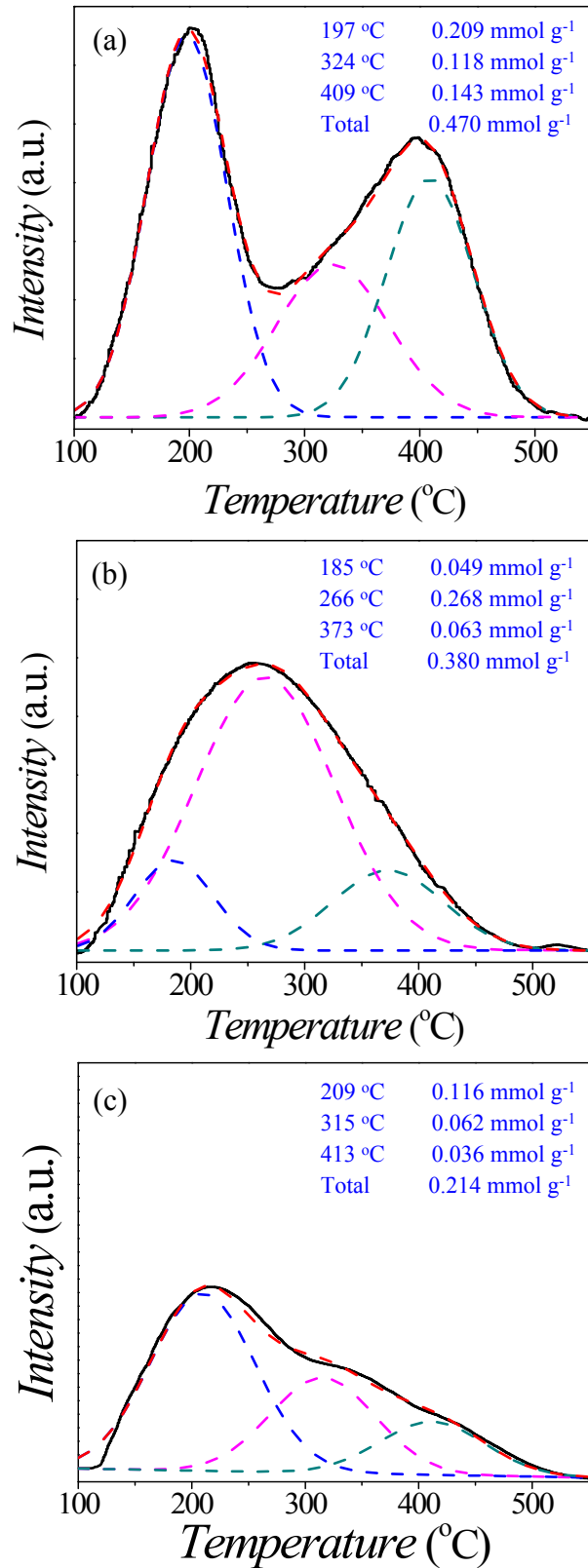


**Fig. S11** NH<sub>3</sub>-TPD profiles of the pristine ZSM-5 (a), ZSM-5@Mg<sub>3</sub>Si<sub>4</sub>O<sub>9</sub>(OH)<sub>4</sub> (b) and MgO/ZSM-5 (c).

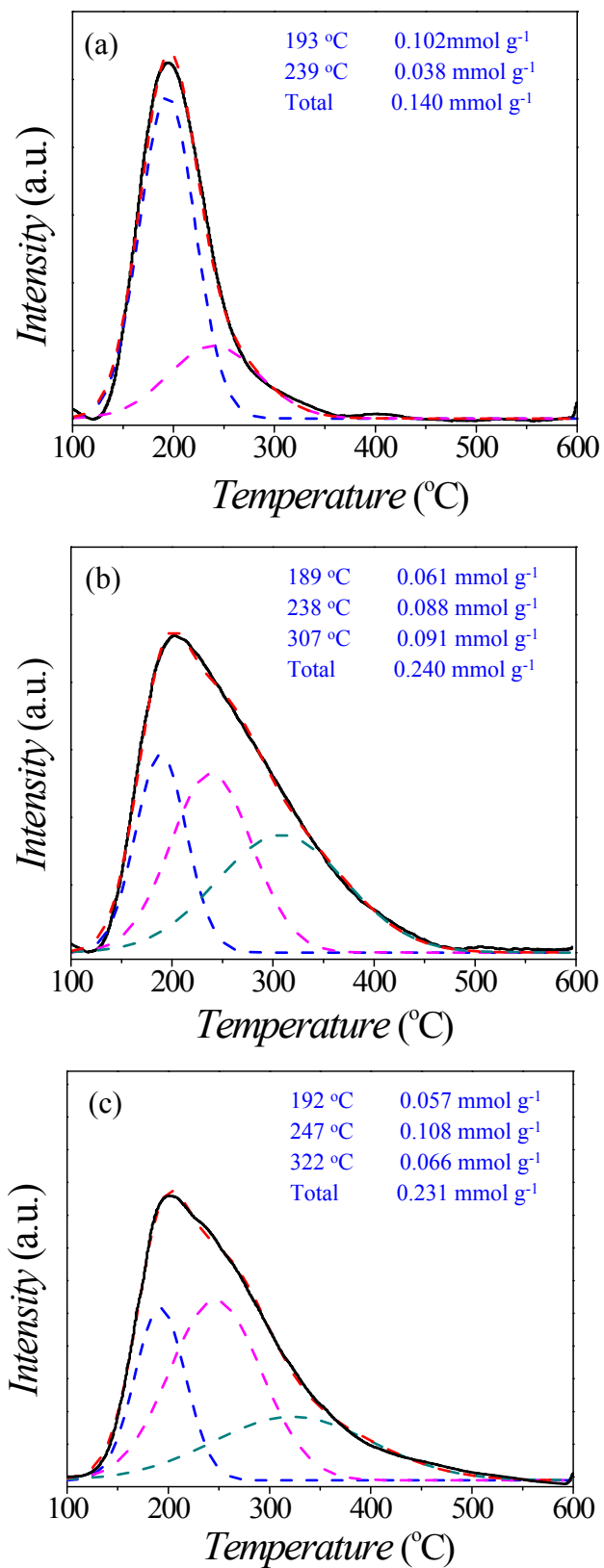


**Fig. S12** CO<sub>2</sub>-TPD profiles of the pristine ZSM-5 (a) and ZSM-5@Mg<sub>3</sub>Si<sub>4</sub>O<sub>9</sub>(OH)<sub>4</sub> (b) and MgO/ZSM-5 (c).

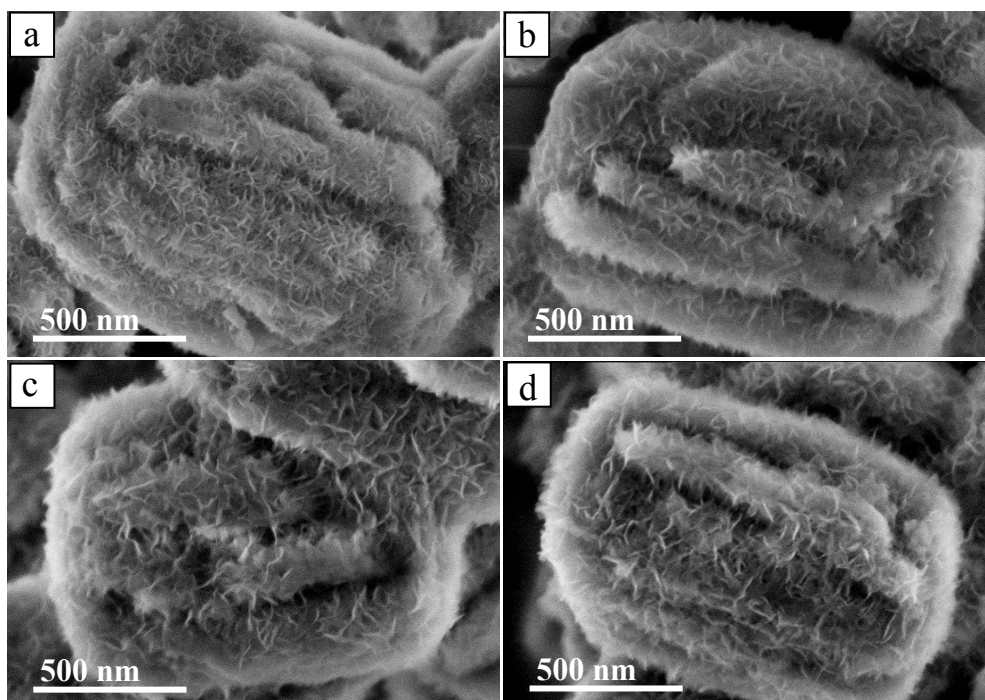


**Fig. S13** SEM images of ZSM-5@Mg<sub>3</sub>Si<sub>4</sub>O<sub>9</sub>(OH)<sub>4</sub> with a magnesium loading of 5.1 wt% (a), 7.6 wt% (b), 10.0 wt% (c), 12.6 wt% (d) and 15.1 wt% (e).

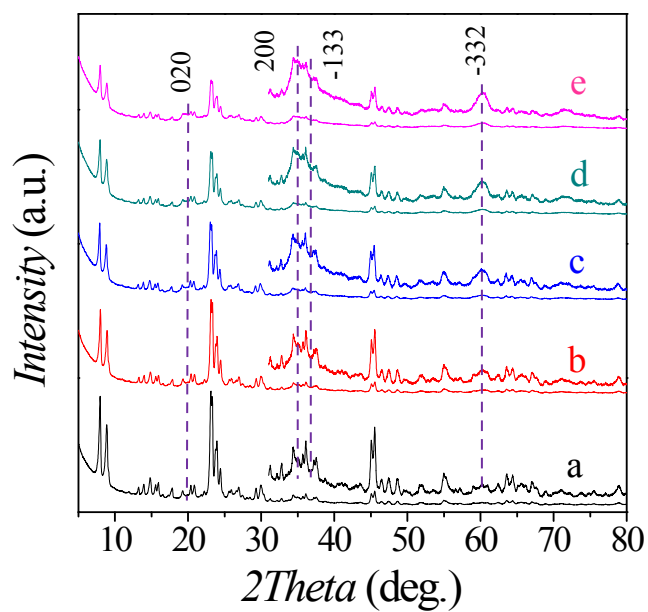


**Fig. S14** XRD patterns of ZSM-5@Mg<sub>3</sub>Si<sub>4</sub>O<sub>9</sub>(OH)<sub>4</sub> with a magnesium loading of 5.1 wt% (a), 7.6

wt% (b), 10.0 wt% (c), 12.6 wt% (d) and 15.1 wt% (e).

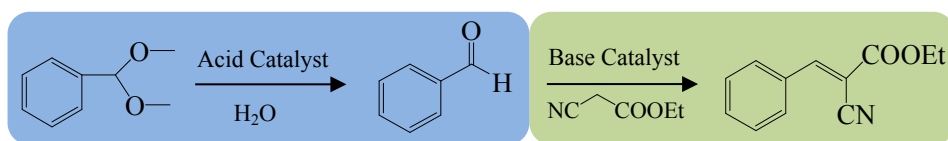


**Fig. S15** The reaction path of one-pot deacetalization-Knoevenagel condensation reaction.

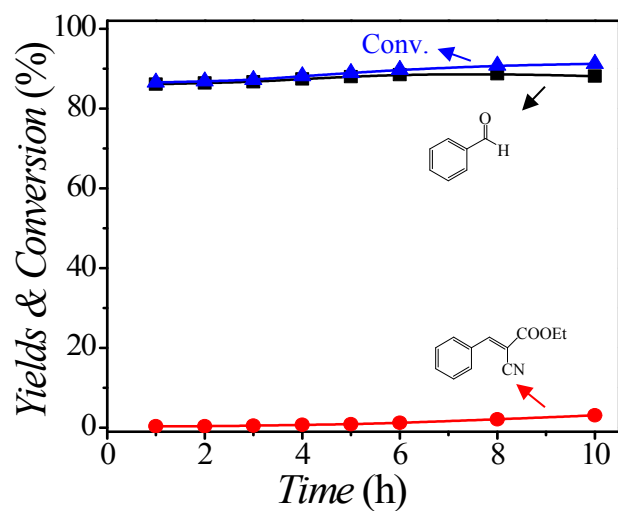


**Fig. S16** The kinetics of one-pot deacetalization-Knoevenagel condensation reaction over the pristine ZSM-5. Reaction conditions: catalyst, 50 mg; benzaldehyde dimethylacetal, 5 mmol; ethyl cyanoacetate, 7.5 mmol; H<sub>2</sub>O, 5 mmol; toluene, 2 mL.

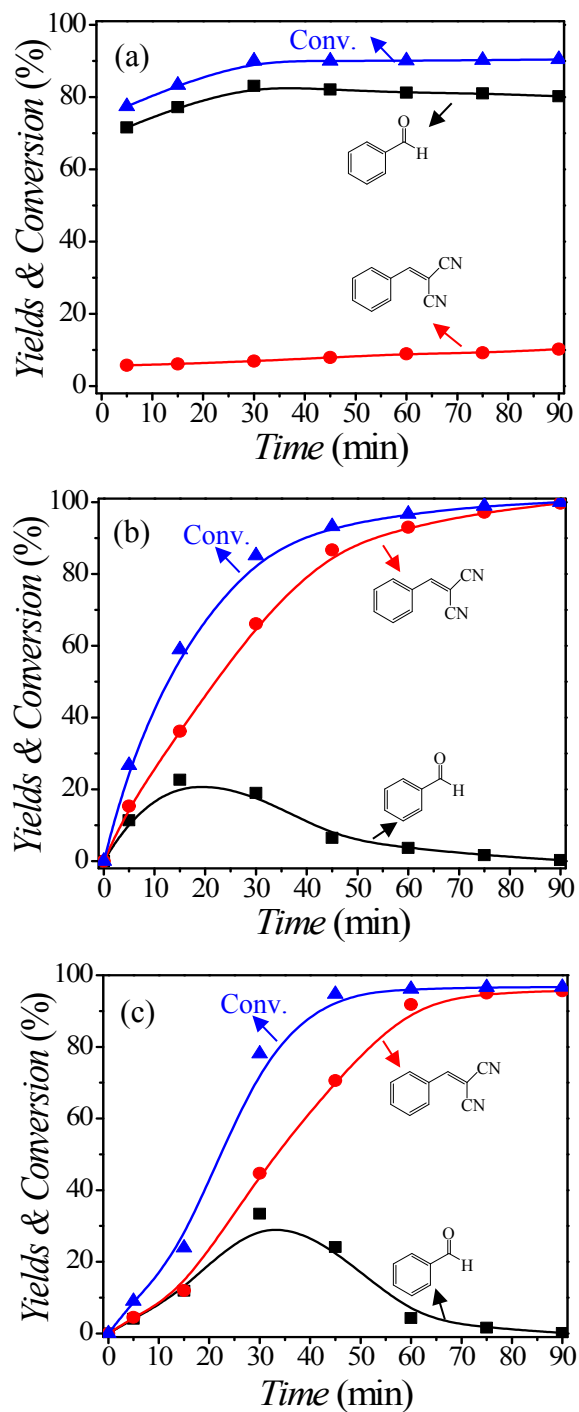


**Fig. S17** The kinetics of one-pot deacetalization-Knoevenagel condensation reaction over the pristine ZSM-5 (a), ZSM-5@Mg<sub>3</sub>Si<sub>4</sub>O<sub>9</sub>(OH)<sub>4</sub> (b) and MgO/ZSM-5 (c). Reaction conditions: catalyst, 50 mg; benzaldehyde dimethylacetal, 5 mmol; malononitrile, 7.5 mmol; H<sub>2</sub>O, 5 mmol; toluene, 2 mL; temp., 90°C.

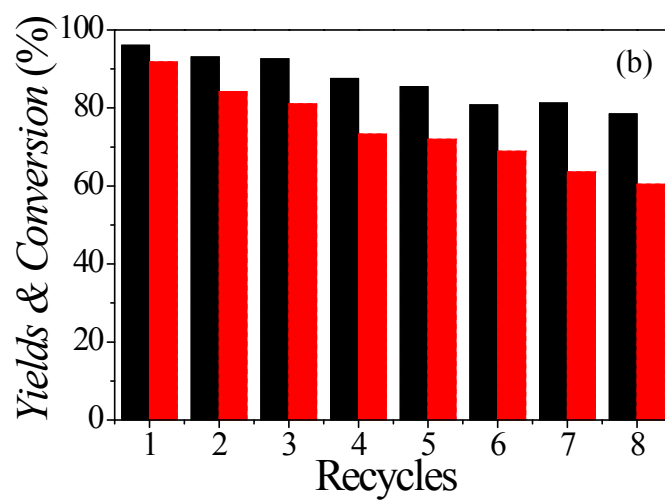
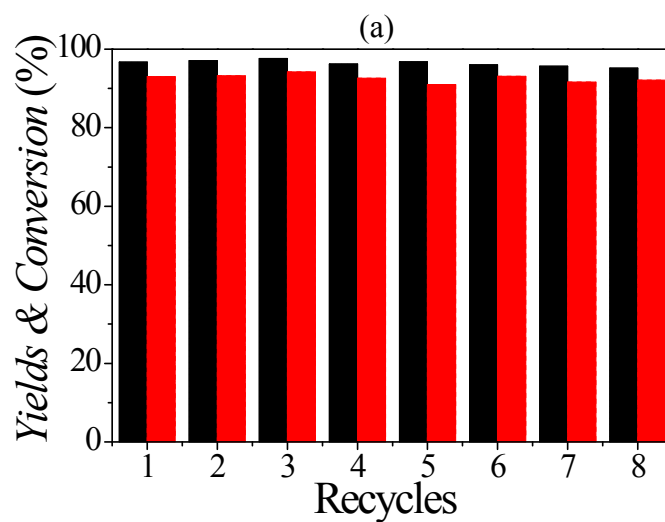


**Fig. S18** Stability tests for the MgSiO<sub>2</sub>/ZSM-5 (a) and MgO/ZSM-5 (b) catalysts. Black column: conversion of benzaldehyde dimethylacetal, red column: yield of benzylidene malononitrile. Reaction conditions: catalyst, 50 mg; benzaldehyde dimethylacetal, 5 mmol; malononitrile, 7.5 mmol; H<sub>2</sub>O, 5 mmol; toluene, 2 mL; temp., 90°C, time, 60 min.

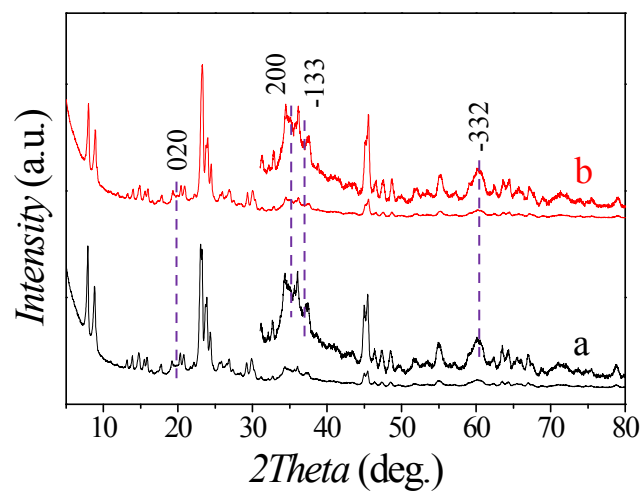


**Fig. S19** XRD patterns of ZSM-5@Mg<sub>3</sub>Si<sub>4</sub>O<sub>9</sub>(OH)<sub>4</sub> before (a) and after (b) using for eight times.

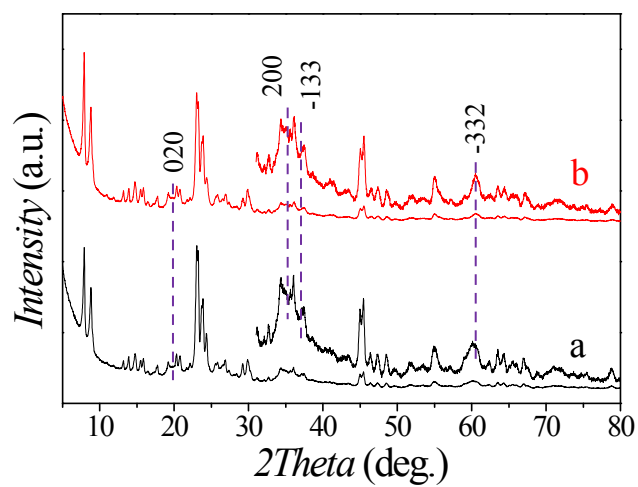


**Fig. S20** XRD patterns of ZSM-5@Mg<sub>3</sub>Si<sub>4</sub>O<sub>9</sub>(OH)<sub>4</sub> before (a) and after (b) calcination at 700 °C for 24 h.

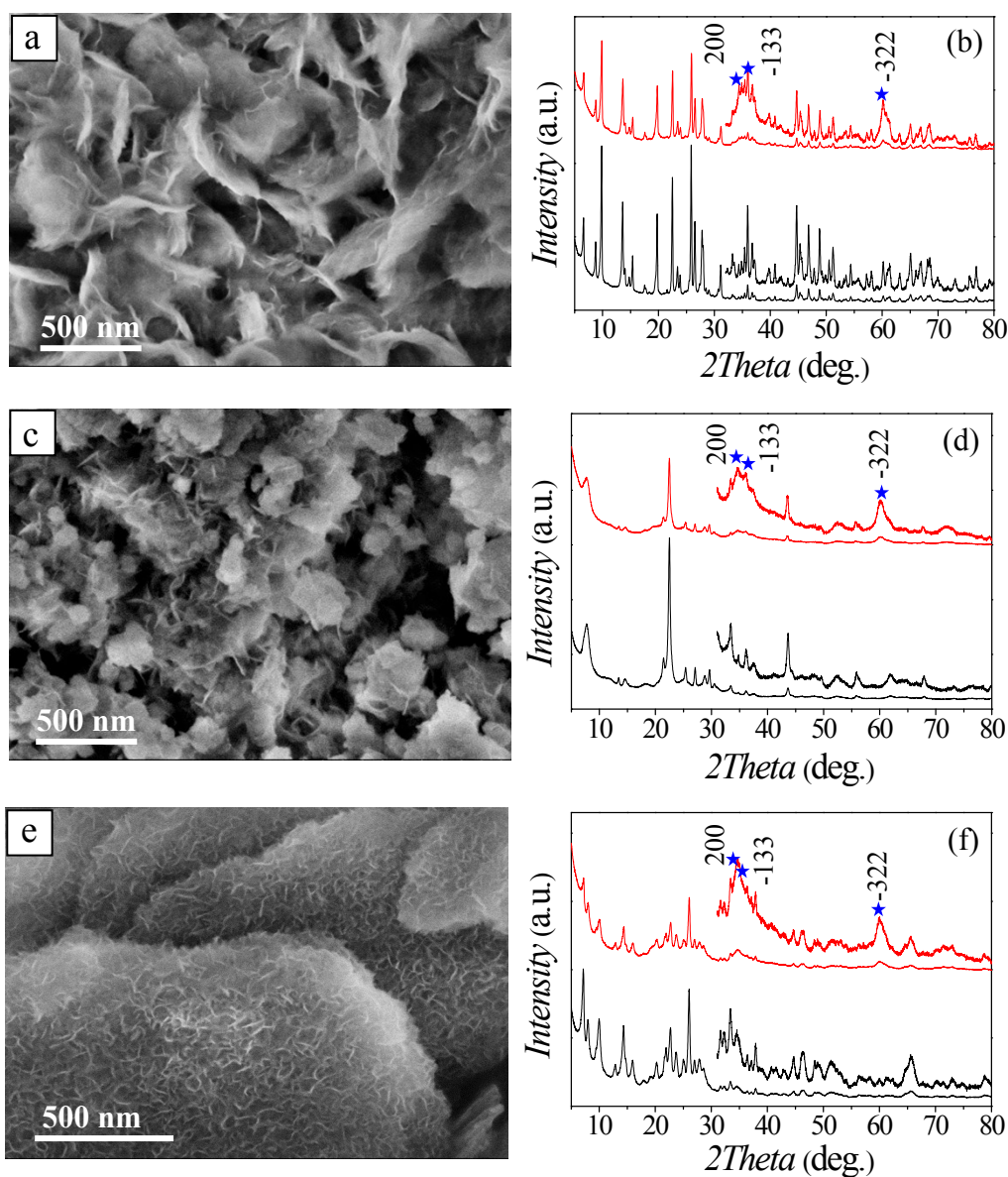


**Fig. S21** SEM images of  $\text{Mg}_3\text{Si}_4\text{O}_9(\text{OH})_4$  coated on different zeolites: mordenite@ $\text{Mg}_3\text{Si}_4\text{O}_9(\text{OH})_4$  (a), Beta@ $\text{Mg}_3\text{Si}_4\text{O}_9(\text{OH})_4$  (c) and MCM-22@ $\text{Mg}_3\text{Si}_4\text{O}_9(\text{OH})_4$  (e). The corresponding XRD patterns were given in (b), (d) and (f), respectively. Black lines were pristine zeolites while red lines were Zeolites@ $\text{Mg}_3\text{Si}_4\text{O}_9(\text{OH})_4$ .

Notably, the Si/Al molar ratio for mordenite, Beta and MCM-22 used in the text were 40, 35 and 42, respectively. Magnesium silicate coated on different zeolites was synthesized by simply varying the types of zeolites added in the hydrothermal reaction solution. SEM images showed all

zeolites were coated with flower-like nanosheets despite the different framework structures. Corresponding to the SEM images, XRD patterns of Zeolites@Mg<sub>3</sub>Si<sub>4</sub>O<sub>9</sub>(OH)<sub>4</sub> showed the weak peaks indexed to magnesium silicate (Mg<sub>3</sub>Si<sub>4</sub>O<sub>9</sub>(OH)<sub>4</sub>, JCPDS No. 03-0174), peaks centered at around 34.5°, 36.2 ° and 60.5° were corresponded to the [200], [-133] and [-332] planes, respectively.<sup>2</sup>

## References

1. D. Wang, L. Xu and P. Wu, *J. Mater. Chem., A*, 2014, **2**, 15535.
2. Y. Wang, G. Wang, H. Wang, C. Liang, W. Cai and L. Zhang. *Chem. -Eur. J.* 2010, **16**, 3497.